

Role of PVP on the Phase Composition and Morphology of Manganese Ferrite Nanoparticles Prepared by Thermal Treatment Method

Mahmoud Goodarz Naseri¹⁺, Elias B. Saion² and Abdul Halim Shaari³

¹Department of Physics, Faculty of Science, Malayer University, Malayer, Iran.

^{1,2,3}Department of Physics, Universiti Putra Malaysia, 43400 UPM Serdang, Selangor, Malaysia.

Abstract. Manganese ferrite nanocrystals were prepared from an aqueous solution containing metal nitrates and various of concentrations of poly(vinyl pyrrolidone) as a capping agent to stabilize the particles and prevent them from agglomerating. To stabilize the particles, they were thermally treated at 873 K as an optimum calcination temperature. The presence of the crystalline phase in each sample was confirmed by X-ray diffraction (XRD) analysis that showed that the presence of the PVP increased the degree of crystallinity of the nanoparticles that were formed. The average particle size and the morphology of the manganese ferrite nanoparticles were determined by transmission electron microscopy (TEM), and these parameters were found to differ with the various concentrations of PVP. Fourier transform infrared spectroscopy (FT-IR) confirmed the presence of metal oxide bands for all of the PVP concentrations and confirmed the absence of organic bands for PVP concentrations less than 0.055 gm/ml.

Keywords: Nanoparticles, Poly(vinyl pyrrolidone), Thermal treatment

1. Introduction

The interest in research related to metal spinel ferrite nanoparticles has increased significantly in recent years due to their potential applications in ferrofluids [1], magnetoptics [2], spintronics [3], biomedical applications [4,5], and anodes for batteries [6]. Various fabrication methods have been reported for preparing spinel ferrite nanocrystals for these purposes, e.g., sol-gel methods [7], the ball-milling technique [8], coprecipitation [9], electrospinning method [10], the hydrothermal method [11], the reverse micelles process [12], and the micro-emulsion method [13]. To overcome the drawbacks associated with the above-mentioned methods, organic and inorganic capping agents are used to stabilize the particles and prevent them from agglomerating. The properties of ferrite nanoparticles can be altered by controlling their size, which can provide an advantage in formulating new composite materials with optimized properties for various applications. Thus, to control the growth of the spinel ferrite nanoparticles, organic stabilizers (polymers), e.g., polyvinyl alcohol (PVA), polyethylene oxide (PEO), polymethacrylic acid (PMAA), and poly(vinyl pyrrolidone) (PVP), are added during the synthesis for capping the surface of the particles [14,15]. In order to avoid the natural tendency to form aggregates, manganese ferrite nanoparticles were normally prepared or dispersed in PVP matrices. Currently, understanding of the effect of capping nanoparticles is one of the most important topics in this area of research. Thus, in this work, the fundamental question that we are attempting to address is how and to what extent the PVP capping agent improves the efficiency of manganese ferrite nanoparticles fabricated by the thermal treatment method.

2. Experimental

Metal nitrate reagents, poly (vinyl pyrrolidone) (PVP), and deionized water were used as precursors. In addition, a capping agent to control the agglomeration of the particles and a solvent were used. Iron nitrate,

⁺ Corresponding author: Tel +60142698153; Fax: +603 89454454
E-mail address: mahmoud.naseri55@gmail.com

$\text{Fe}(\text{NO}_3)_3 \cdot 9\text{H}_2\text{O}$, and manganese nitrate, $\text{Mn}(\text{NO}_3)_2 \cdot 6\text{H}_2\text{O}$, were purchased from Acros Organics with a purity exceeding 99%. PVP (MW = 29000). In the next set of experiments, we synthesized four separate aqueous solution of PVP were prepared by dissolving 0, 1.5, 4 and 5.5 g of polymer in 100 ml of deionized water at 363 K, before mixing 0.2 mmol iron nitrate and 0.1 mmol manganese nitrate (Fe:Mn = 2:1) into the polymer solution and constantly stirring for 2 h using a magnetic stirrer until a colorless, transparent solution was obtained. The mixed solution was poured into a glass Petri dish and heated at 353 K in an oven for 24 h to evaporate the water. The dried, orange, solid manganese ferrite that remained was crushed and ground in a mortar to form powder. The calcination of the powders was conducted at 873 K for 3 h for the decomposition of organic compounds and the crystallization of the nanocrystals.

3. Characterization

The structure of the MnFe_2O_4 nanoparticles was characterized by the XRD technique using a Shimadzu diffract meter model XRD 6000 employing $\text{Cu K}\alpha$ (0.154 nm) radiation to generate diffraction patterns from powder crystalline samples at ambient temperature in a 2θ range of 10° to 70° . The microstructure and particle size of the nanocrystals were determined from Transmission Electron Microscopy (TEM) images that were obtained by using a JEOL 2010F UHR version electron microscope at an accelerating voltage of 200 kV. FT-IR spectra were recorded using a PerkinElmer FT-IR model 1650 spectrometer. Before recording spectra, the samples were placed on a Universal ATR Sampling Accessory (diamond coated with CsI) and pressed, and then the spectra were recorded.

4. Results and Discussion

Interactions between the PVP capping agent [16] and metal ions are shown schematically in Figure 1, which shows that the manganese (II) and iron (III) ions are bound by the strong ionic bonds between the metallic ions and the amide group in a polymeric chain. PVP acts as a stabilizer for dissolved metallic salts through steric and electrostatic stabilization of the amide groups of the pyrrolidine rings and the methylene groups. Initially, the PVP stabilizer may decompose to as limited extent, thereby producing shorter polymer chains that are capped when they are adsorbed onto the surfaces of metallic ions [17]. The metallic ions, which are well dispersed in the cavities and networks, are created as a result of the shorter polymer chains. These mechanisms continue until they are terminated by the drying step. The influence of PVP is not restricted only to the solution and the drying step; PVP also affects the formation of the nuclei (i.e., nucleation) of the manganese ferrite nanoparticles in the calcination step. In this step, the small nanoparticles with high surface energy levels would become larger via the Ostwald ripening process [18] without the presence of PVP, disrupts steric hindrance, thereby preventing their aggregation. Steric hindrance is a phenomenon that is attributed to large molecular weight (>10,000) and the repulsive forces acting among the polyvinyl groups [19, 20]. These interactions are similar to the stabilization of metallic nanoparticles, i.e., silver and gold [21, 22]

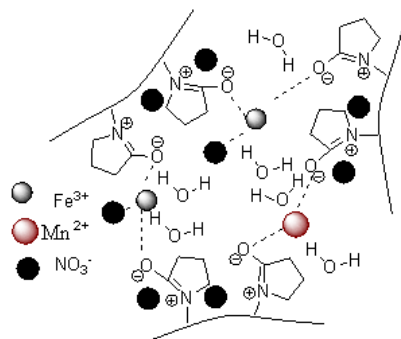


Fig. 1:

Fig. 2 shows the XRD peaks of manganese ferrite nanoparticles that were prepared with concentrations of PVP, ranging from 0 to 0.055 g/ml, and calcined at 873 K. It is important to note that, in thermal treatment method, the optimum temperature for the calcination of manganese ferrite nanoparticles was 873 K, because

this temperature was the minimum temperature at which the nanoparticles were pure; also, this is the temperature at which the nanoparticles have the smallest particle size and a nearly uniform distribution of shapes [16]. It is evident from Figure 2 that the patterns show the reflection planes (111), (220), (311), (222), (400), (331), (422), (511), and (440), which confirm the presence of single-phase MnFe_2O_4 with a face-centered cubic structure [23]. Except for the impure phase of $\alpha\text{-Fe}_2\text{O}_3$, which is found in all calcined samples and occur naturally as hematite [24], the remaining peaks correspond to the standard pattern of MnFe_2O_4 (cubic, space group: $\text{Fd}\bar{3}\text{m}$, $Z = 8$; ICDD PDF: 73-1964). A comparison of XRD peaks shows that either the numbers or the intensities of the unwanted peaks of $\alpha\text{-Fe}_2\text{O}_3$ increase in the absence of PVP, but when PVP is present at concentrations of 0.015, 0.04 and 0.055 g/ml, either remove some of the unwanted peaks of $\alpha\text{-Fe}_2\text{O}_3$ or decrease the intensities of the some of them. This could be due to the fact that decreasing the concentration of PVP results in increases in the concentrations of manganese and iron ions [25]. In fact, due to the absence of PVP, there is no interaction between ferrite and PVP chains, which resulted in increasing either the numbers or the intensities of the unwanted peaks of $\alpha\text{-Fe}_2\text{O}_3$ [26]. Therefore, one of the important roles of PVP in synthesis of manganese ferrite nanoparticles by the thermal treatment method is the enhancement of the degree of the crystallinity by decreasing or removing $\alpha\text{-Fe}_2\text{O}_3$.

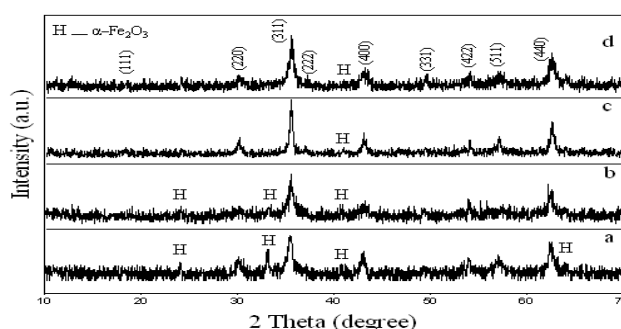


Fig. 2:

To further investigate the role of PVP in the synthesis of manganese ferrite nanoparticles, we have shown, the TEM images and the FT-IR spectra of manganese ferrite nanoparticles with various of concentrations of 0, 0.015, 0.04 and 0.055 g/ml (Fig. 3 and 4). Figure 3a shows that manganese ferrite nanoparticles were formed even in the absence of PVP. However, in this case, it was observed that the nanoparticles did not have a uniform distribution of shapes, and they were aggregated extensively and, in some areas, completely disproportionately distributed. Thus, without the use of PVP in the synthesis of nanoparticles, the small nanoparticles aggregate and produce larger nanoparticles [20] due to high surface energy (as shown earlier in Fig. 1). When the concentration of PVP was increased to 0.015 g/ml, the manganese ferrite nanoparticles that were formed with average size of 20 nm became more regular in shape than in the case without PVP (Fig. 3b). But, due to the low concentration of PVP, these nanoparticles also aggregated because there was insufficient PVP to cap them well and prevent their agglomeration. By increasing the PVP concentration to 0.055 g/ml, the manganese ferrite nanoparticles did not agglomerate, and they were nearly uniform in shape, as shown in Figure 3d. However, in this case, the manganese ferrite nanoparticles ranged in size from 17 to 27 nm, with an estimated average particle size of 22 nm. These results were similar to the results achieved when a PVP concentration of 0.04 gm/ml was used (shown in Fig. 3c).

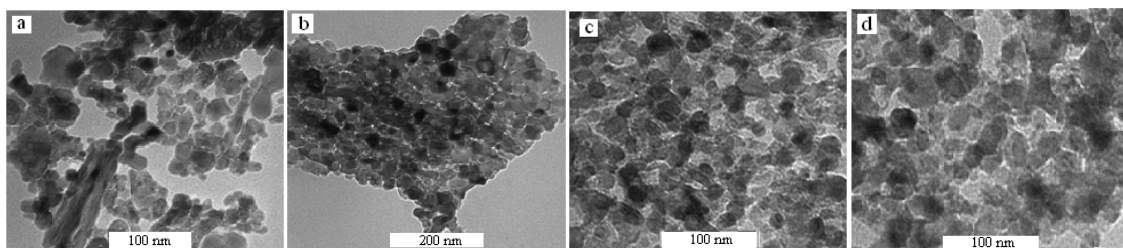


Fig. 3:

Two main broad metal–oxygen bands are seen in Figure 4 in the IR spectra of all spinel ferrite nanoparticles, which correspond to intrinsic stretching vibrations of the metal at the tetrahedral site, $M_{\text{tetra}} \leftrightarrow O$ (observed from 519 to 556 cm^{-1}) and octahedral-metal stretching, $M_{\text{octa}} \leftrightarrow O$ (observed from 403 to 429 cm^{-1}) [27]. But, due to the high concentration of PVP, traces of organic materials were observed at 1668 cm^{-1} which was associated with C=O stretching vibration respectively [28] as shown in Figure 4d. So, in fact, it is apparent that the manganese ferrite nanoparticles were contaminated with organic compounds in this case. But in the absence of PVP and with concentrations of less than 0.055 g/ml, the fabricated manganese ferrite nanoparticles were pure as shown in Figures 4a, 4b and 4c. Therefore, in the thermal treatment method, the optimum concentration of PVP for the synthesis of manganese ferrite nanoparticles is 0.04 gm/ml. That concentration, in combination with the optimum temperature (873 K) provided the conditions required to fabricate pure manganese ferrite nanoparticles that have the smallest particle size.

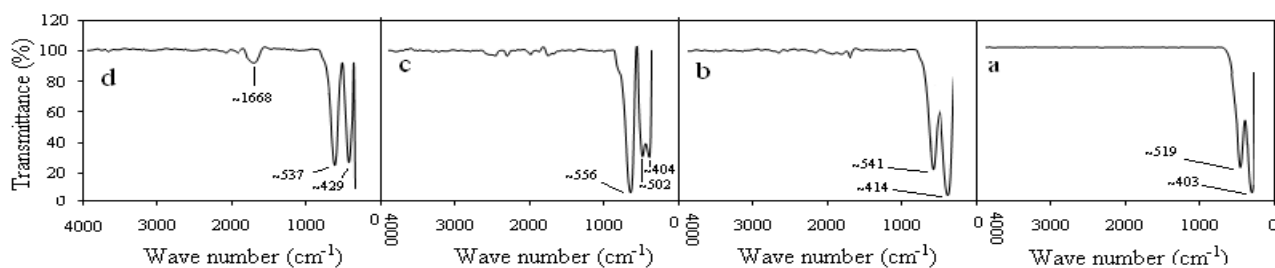


Fig. 4:

5. Conclusion

We concluded that the effect and role of PVP in the synthesis of manganese ferrite nanoparticles by the thermal treatment method is astonishing. Briefly, as was discussed when we considered our XRD results, TEM images, and FT-IR spectra, PVP plays four crucial roles in synthesizing manganese ferrite nanoparticles, i.e., (1) the control of the growth of the nanoparticles; (2) the prevention of agglomeration of the nanoparticles; (3) the enhancement of the degree of the crystallinity of the nanoparticles, and (4) the production of nanoparticles that have a uniform distribution of shapes.

6. Acknowledgment

This work was supported by the Ministry of Higher Education of Malaysia under the FRGS grant and Universiti Putra Malaysia under the RUGS grant and Malayer university in Iran.

7. References

- [1] Rosesweig R E (1985) Ferrohydrodynamics. Dover New York, USA.
- [2] Tirosh E, Shemer G, Markovich G, (2006) Optimizing Cobalt Ferrite Nanocrystal Synthesis Using a Magneto-Optical Probe. Chem Mater 18: 465-470.
- [3] Luders U, Barthelemy A, Bibes M, (2006) NiFe₂O₄: A versatile spinel magterial brings new opportunities for Spintronics. Adv Mater 18: 1733-1736.
- [4] Pankhurst Q A , Connolly J , Jones S K (2003) Applications of magnetic nanoparticles in biomedicine. J Phys D: Appl Phys 36: R167-R181.
- [5] Berry C C (2005) Possible exploitation of magnetic nanoparticles-cell interaction for biomedical applications J. Mater. Chem 15: 543-547.
- [6] Selvan R K, Kalaiselvi N, Augustin C O (2006) SnO₂ pinning: an approach to enhance the electrochemical properties of anodes for batteries. Electrochem Solid State Lett 9: A390–394.
- [7] Atif M, Hasanian S K, and Nadeem M (2006) Magnetization of sol-gel prepared zinc ferrite nanoparticles: Effects of inversion and particle size. Solid State Commun. 138: 416-421.
- [8] Jiang J Z, Wynn P, Morup S (1999) Magnetic structure evolution in mechanically milled nanostructured ZnFeO₂ particles. Nanostruct Mater 12: 737-740.

- [9] Shenoy S D, Joy P A, Anantharaman M R (2004) Effect of mechanical milling on the structural, magnetic and dielectric properties of coprecipitated ultrafine zinc ferrite. *J Magn Magn Mater* 269: 217-226.
- [10] Maensiri S Sangmanee M Wiengmoon A (2009) Magnesium Ferrite (MgFe₂O₄) Nanostructures Fabricated by Electrosinning. *Nanoscale Res Lett* (2009) 4:221–228.
- [11] Yu S H, Fujino T, Yoshimura M (2003) Hydrothermal Synthesis of ZnFe₂O₄ Ultrafine Particles with High Magnetization. *J Magn Magn Mater* 256: 420-427.
- [12] Morrison S A , Cahill C L , Carpenter E E (2004) Magnetic and Structural Properties of Nickel Zinc Ferrite Nanoparticles Synthesized at Room Temperature. *J Appl Phys* 95: 6392- 6395.
- [13] Hocheplied J P, Bonville J F, and Pileni, M P (2000) Non stoichiometric Zinc Ferrite nanocrystals: Syntheses and magnetic properties. *J Phys Chem* 104: 905-912.
- [14] Rana S, Gallo A, Srivastava R S (2007) On the suitability of nanocrystalline ferrites as a magnetic carrier for drug delivery: Functionalization, conjugation, and drug release behavior. *Acta Biomaterialia* 3: 233-242.
- [15] Naseri M G, Saion E B , Abbastabar A H Hashim M Shaari A H (2011) Simple preparation and characterization of nickel ferrite nanocrystals by a thermal treatment method. *Powder Technol* 212: 80–88.
- [16] Sivakumar P, Ramesh R, Ramanand A (2011) Synthesis and characterization of NiFe₂O₄ nanosheet via polymer assisted co-precipitation method. *Mater Lett* 65: 483-485.
- [17] Koebel M M, Louis C, Jones and Gabor A S (2008) Preparation of size-tunable, highly monodisperse PVP-protected Pt-nanoparticles by seed-mediated growth. *J Nanopart Res* 10: 1063-1069.
- [18] Roosen A R, Carter W C (1998) Simulations of microstructural evolution: Anisotropic growth and coarsening. *Physica A* 261: 232-247.
- [19] Ghosh G , Naskar M K, Patra A (2006) Synthesis and characterization of PVP-encapsulated ZnS nanoparticles. *Opt Materi* 28: 1047-1053.
- [20] Shao H, Hi Y, Lee H (2006) Effect of PVP on the morphology of 1 cobalt nanoparticles prepared by thermal decomposition of cobalt acetate. *Curr Appl Phy* 6: e195-e197.
- [21] Wen-yao H and Guo.-cai X (2010) Characterization of nano-Ag/PVP composites synthesized via ultra-violet irradiation. *J Coal Sci Eng* 16: 188-192.
- [22] Tsuji M, Hashimoto M , Nishizawa Y, Tsuji T (2004) Synthesis of gold nanorods and nanowires by microwave-polyol method. *Mater Lett* 58 : 2326-2330.
- [23] Singh J P, Sirvastava R C, Agrawal H M, and Kushwaha R P S (2009) 577 Fe Mössbauer spectroscopic study of nanostructured zinc ferrite. *Hyperfine Interactions* 183(1-3): 221-228.
- [24] Laokul P, Amornkitbamrung V, Seraphin S (2011) Characterization and magnetic properties of nanocrystalline CuFe₂O₄, NiFe₂O₄, ZnFe₂O₄ powders prepared by the Aloe vera extract solution. *Curr Appl Phy* 11: 101-108.
- [25] Cullity B D (1987) *Elements of X-Ray Diffraction*. Addison-Wesley London UK.
- [26] Sharma D R , Mathur R, Vadera S R (2003) Synthesis of nanocomposites of Ni–Zn ferrite in aniline formaldehyde copolymer and studies on their pyrolysis products. *J. Alloys Compd.* 358: 193-204.
- [27] Elsayed A H, Mohy Eldin M S, Elsyed A M (2011) Synthesis and Properties of Polyaniline/ferrites Nanocomposites. *Int J Electrochem Sci* 6: 206-221.
- [28] Hunyek A Sirisathikul C and Harding P (2011) Formation of cobalt ferrites from aqueous solutions of metal nitrates containing PVA: effects of the amount of PVA and annealing temperature. *J Ceram Soc Jpn* 119: 541-544.